

April 2018

## **Empirical Modeling of Cation Ordering in Perovskite Ceramics**

Evan Smith  
*Boise State University*

Kevin Tolman  
*Boise State University*

Rick Ubic  
*Boise State University*

---

## Empirical Modeling of Cation Ordering in Perovskite Ceramics

### Abstract

The electroceramics industry largely relies on various time-consuming and expensive trial-and-error experiments to address new questions which often could otherwise be interpolated from published data. Towards this end, predictive models, which can be derived from empirical evidence, can greatly aid the direction of future development in a meaningful and cost-effective way. This work focuses on deriving predictive models based on empirical data collected for ceramic compounds with the perovskite crystal structure. Specifically, models were made for layered type ordering in the  $[(\text{Na}_y\text{Li}_{1-y})(1-3x)/2\text{La}_{(1+x)/2}]\text{TiO}_3$  system and rocksalt ordering in  $\text{Ba}(\text{Mg}_{1/3}\text{Ta}_{2/3})\text{O}_3$ .



# Empirical Modeling of Cation Ordering in Perovskite Ceramics

BOISE STATE UNIVERSITY

COLLEGE OF ENGINEERING

MICRON SCHOOL OF MATERIALS SCIENCE AND ENGINEERING

Evan Smith, Kevin Tolman,\* Rick Ubic

Micron School of Materials Science and Engineering, Boise State University

\* Current address: Idaho National Laboratory

## Abstract

The electroceramics industry largely relies on various time-consuming and expensive trial-and-error experiments to address new questions which often could otherwise be interpolated from published data. Towards this end, predictive models, which can be derived from empirical evidence, can greatly aid the direction of future development in a meaningful and cost-effective way. This work focuses on deriving predictive models based on empirical data collected for ceramic compounds with the perovskite crystal structure. Theory suggests that intrinsic properties on the scale of a unit cell may be estimated from the sizes and charges of the chemical constituents alone. Ultimately, researchers could be provided a compositional recipe for some desired structure/property; or the resulting structure/property could be readily calculated based on composition. Empirical models also lend themselves to the exploration of structure/property trends which would otherwise be virtually impossible to discover via computationally expensive first-principles methods. In this work, models were made for layered ordering in the  $[(\text{Na}_y\text{Li}_{1-y})_{(1-3x)/4}\text{La}_{(1+x)/2}]\text{TiO}_3$  (NLLT) system and rocksalt ordering in  $\text{Ba}(\text{Mg}_{1/3}\text{Ta}_{2/3})\text{O}_3$  (BMT).

## Perovskites

The term “perovskite” defines a particular crystal structure shown in figure 1. The A and B cations and X anions are located at the corners, body center, and face centers, respectively; and anion octahedra are corner-shared. Even when deformed and noncubic, a pseudocubic lattice constant can be derived in several ways:

$$a_{pc} = \left(\frac{V}{Z}\right)^{1/3}$$
$$\begin{aligned} \blacktriangleleft\blacktriangleright a'_{pc} &= \sqrt{2}(r_A + r_X) \\ \blacktriangleleft\blacktriangleright a''_{pc} &= 2(r_B + r_X) \end{aligned}$$

where  $V$  = unit-cell volume;  $Z$  is the number of  $\text{ABX}_3$  formula units per unit cell; and  $r_A$ ,  $r_B$ , and  $r_X$  are the effective radii of A, B, and X species, respectively.

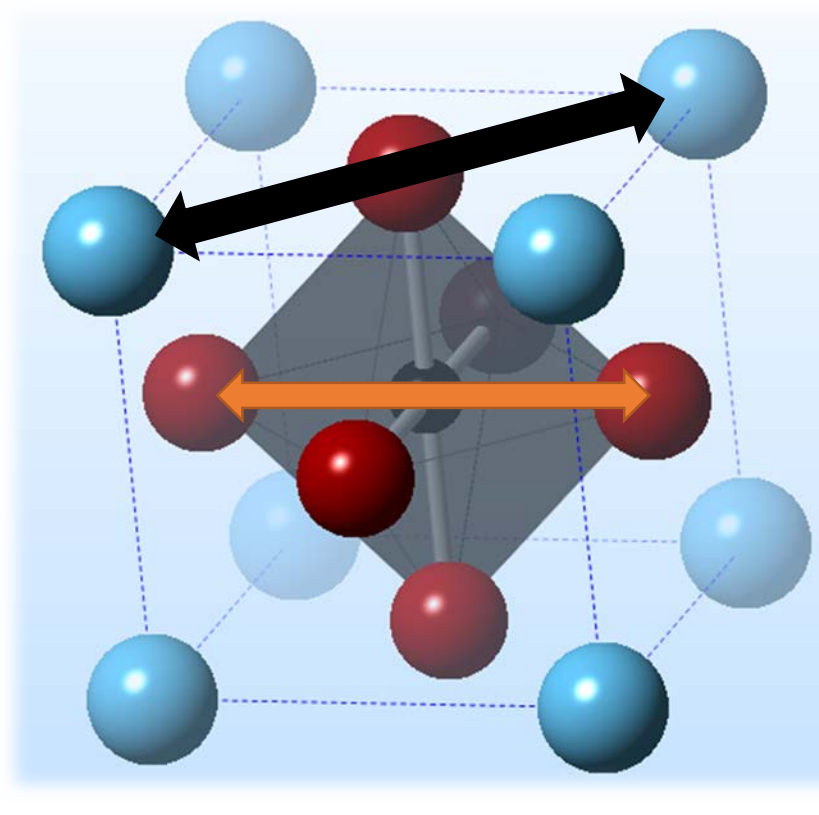


Figure 1: Perovskite crystal structure with arrows indicating the derivation of  $a'$  (black) and  $a''$  (orange)

[1] R. Ubic, K. Tolman, K. Talley, B. Joshi, J. Schmidt, E. Faulkner, J. Owens, M. Papac, A. Garland, C. Rumrill, K. Chan, N. Lundy, H. Kungl, Lattice-constant prediction and effect of vacancies in aliovalently doped perovskites, J. Alloys Compd. 644 (2015) 982-995. [2] K. Tolman, R. Ubic, B. Liu, I. Williamson, K. Bedke, E. Nelson, L. Li, X. Chen, Empirical evidence for A-site order in perovskites, J. Am. Ceram. Soc. 100 (2017) 429-442.

## Methods

Stoichiometric powders were milled in deionized water (Figs. 2 and 3), dried in the drying oven (Fig. 4), and calcined at 1100-1200°C (Fig. 5). Phase purity was verified via X-ray diffraction (XRD). Phase-pure powders of  $[(\text{Na}_y\text{Li}_{1-y})_{(1-3x)/4}\text{La}_{(1+x)/2}]\text{TiO}_3$  (NLLT) and  $\text{Ba}(\text{Mg}_{1/3}\text{Ta}_{2/3})\text{O}_3$  (BMT) were uniaxially pressed into pellets (Fig. 6). NLLT pellets were sintered on a bed of sacrificial powder on the lid of an inverted crucible at 1300-1400°C (Fig. 7). BMT pellets and some unpressed powders were subjected to each of six heat treatments: 5, 10, 15, 20, 30 or 40 hours at 1500°C. Lattice parameters were obtained from Rietveld refinements performed on the XRD scans of sintered powders using GSAS II.



Figure 2 : Mill pot and milling media



Figure 3 : Rotary mill with mill pot



Figure 4 : Drying pan in drying oven



Figure 5 : Crucible in box furnace chamber



Figure 6 : Uniaxial pellet press



Figure 7 : Inverted crucible with sintered pellets

## Results

B-site ordering data from  $\text{Ba}(\text{Mg}_{1/3}\text{Ta}_{2/3})\text{O}_3$  (BMT) are presented in figures 8-9. A-site ordering data from  $(\text{Na}_y\text{Li}_{1-y})_{(1-3x)/4}\text{La}_{(1+x)/2}\text{TiO}_3$  (NLLT) are presented in figures 10-12.

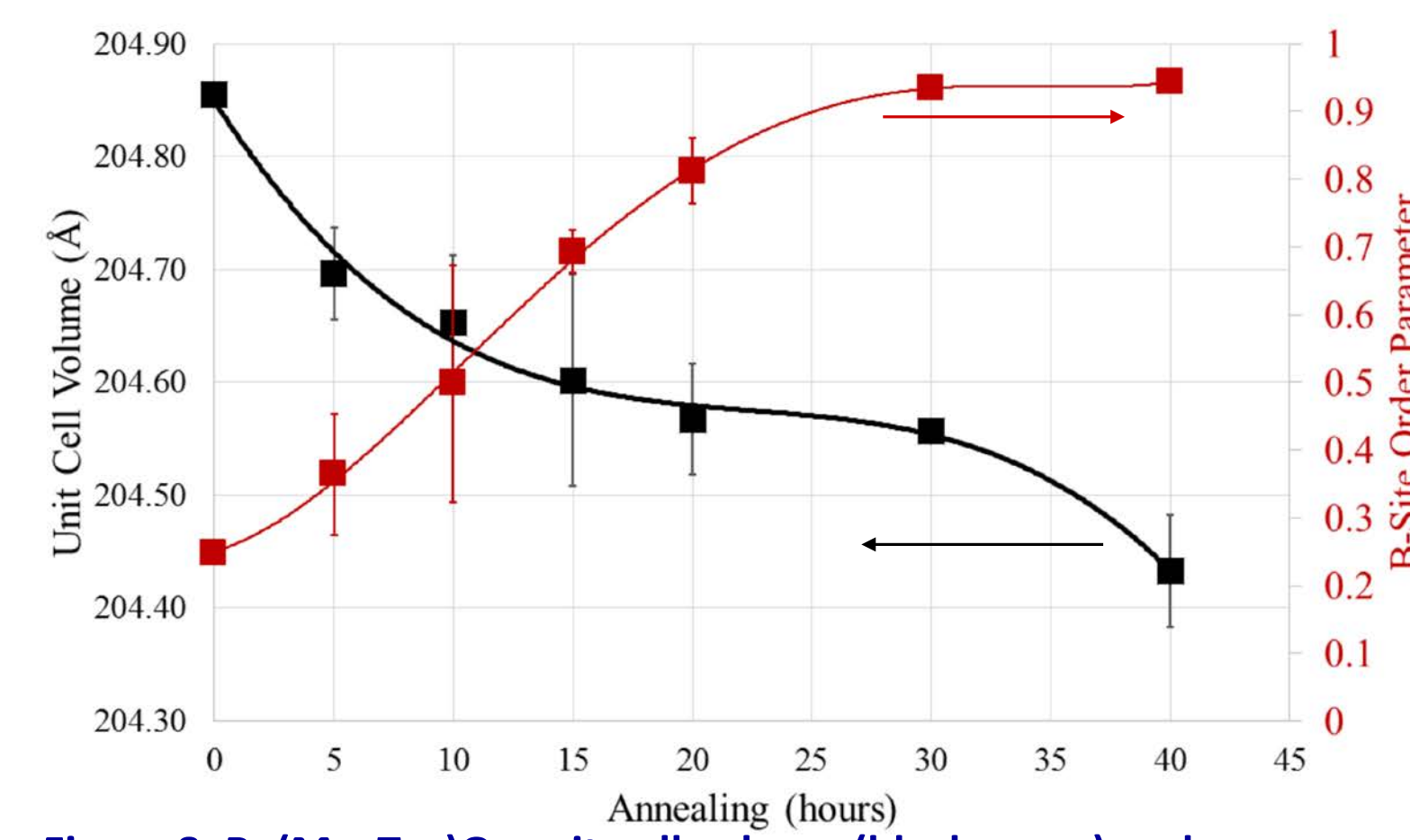


Figure 8:  $\text{Ba}(\text{Mg}_{1/3}\text{Ta}_{2/3})\text{O}_3$  unit-cell volume (black curve) and order parameter (red curve) as a function of annealing time,  $t$ .

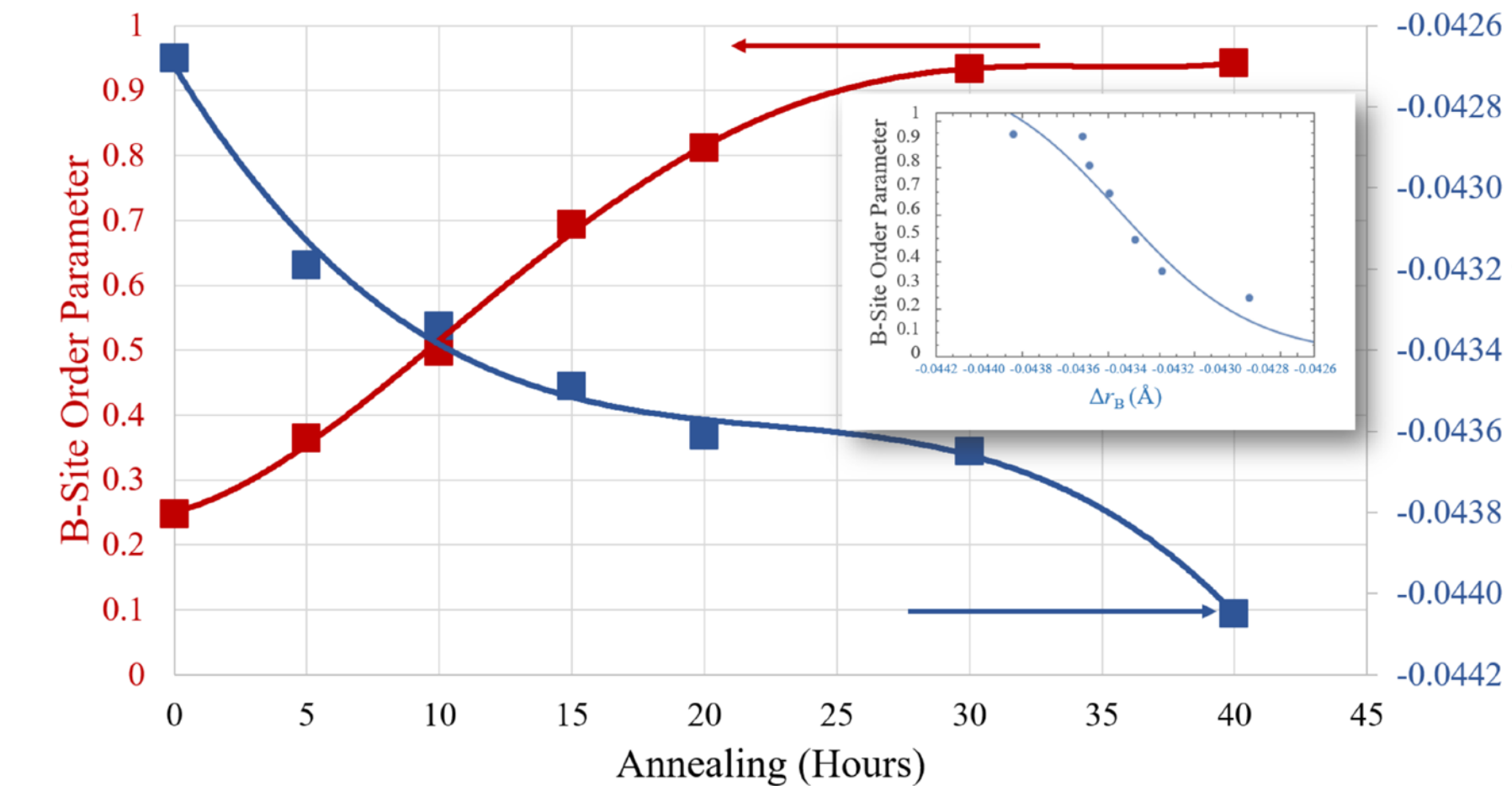


Figure 9:  $\text{Ba}(\text{Mg}_{1/3}\text{Ta}_{2/3})\text{O}_3$  order parameter (red curve) and B-site size adjustment (blue curve) as a function of annealing time,  $t$ . The inset shows the order parameter as a function of  $\Delta r_B$  and can be thought of as an empirical model for ordering (0 = disorder, 1 = fully ordered).

$$1.) Vol = 204.85 - 0.0332t + 0.0014t^2 - 2 \times 10^{-5}t^3 \quad (R^2 = 0.9917)$$
$$3.) \eta = \frac{0.973062}{1 + \exp\left(\frac{8.72456 - t}{7.37166}\right)} \quad (R^2 = 0.9989)$$

$$2.) \Delta r_B = -0.0427 - 0.0001t + 5 \times 10^{-6}t^2 - 7 \times 10^{-8}t^3 \quad (R^2 = 0.9952)$$
$$4.) \eta = \frac{1.22869}{1 + \exp\left(\frac{0.0434304 + \Delta r_B}{3.83894 \times 10^{-4}}\right)}$$

In the case of layered ordering on the A site, Figs. 10 and 11 show that increased ordering results in a volume expansion, requiring a positive  $\Delta r_A$  term. Eq. 5 describes this effect; and the  $a$ ,  $b$ , and  $c$  terms are determined by the blue curves in Fig. 12. Eq. 6 describes  $\eta$  as a function of  $\Delta r_A$  where  $A$ ,  $B$ , and  $C$  are determined by the red curves in Fig. 12. Both volume expansion and contraction can be explained in terms of crystal chemistry.

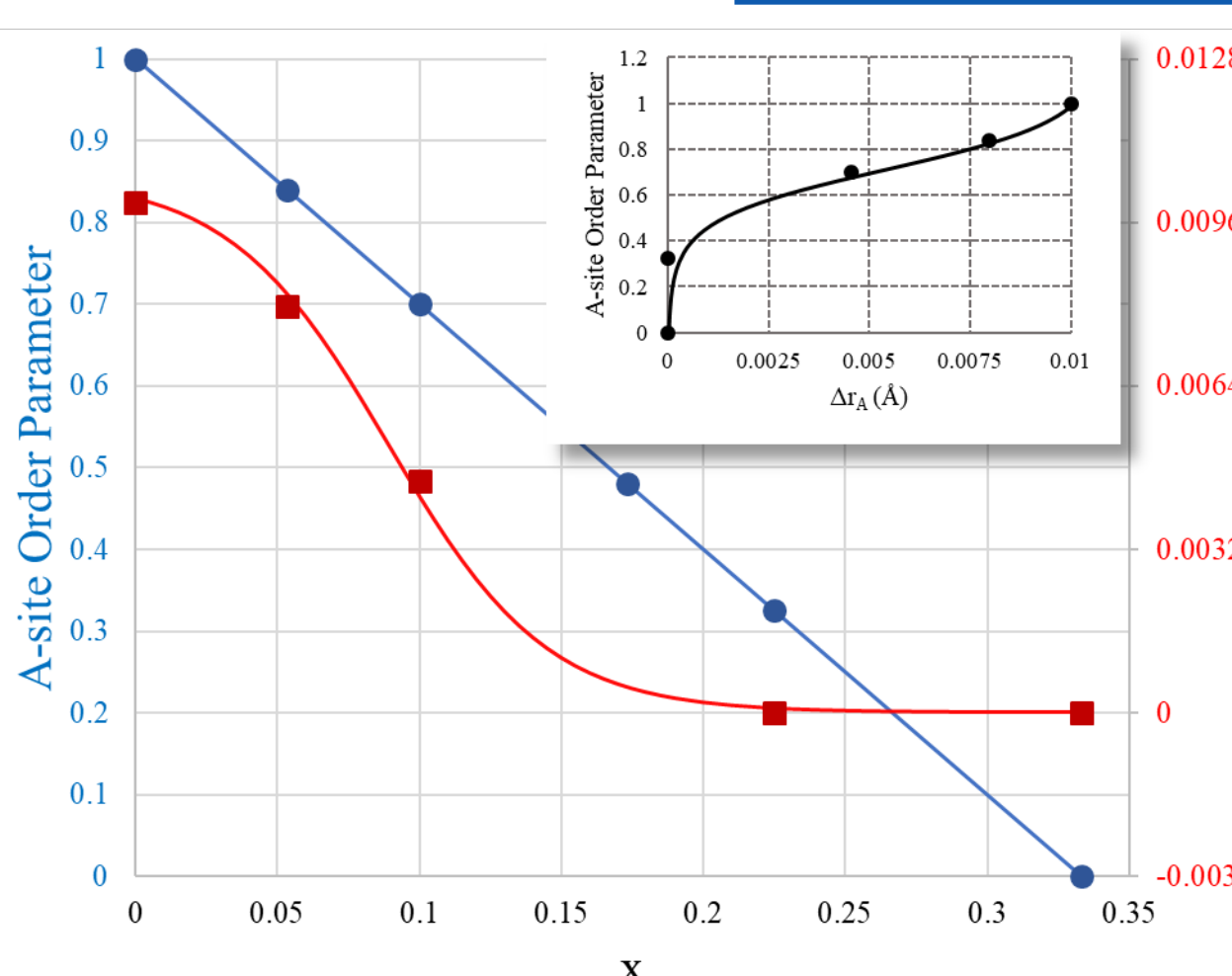


Figure 10:  $\text{Na}_{(1-3x)/4}\text{La}_{(1+x)/2}\text{TiO}_3$  ordering from experimental site occupancies. Inset shows the order parameter as a function of  $\Delta r_A$  (Å) and can be thought of as an empirical model for ordering (0=disordered, 1=fully ordered).

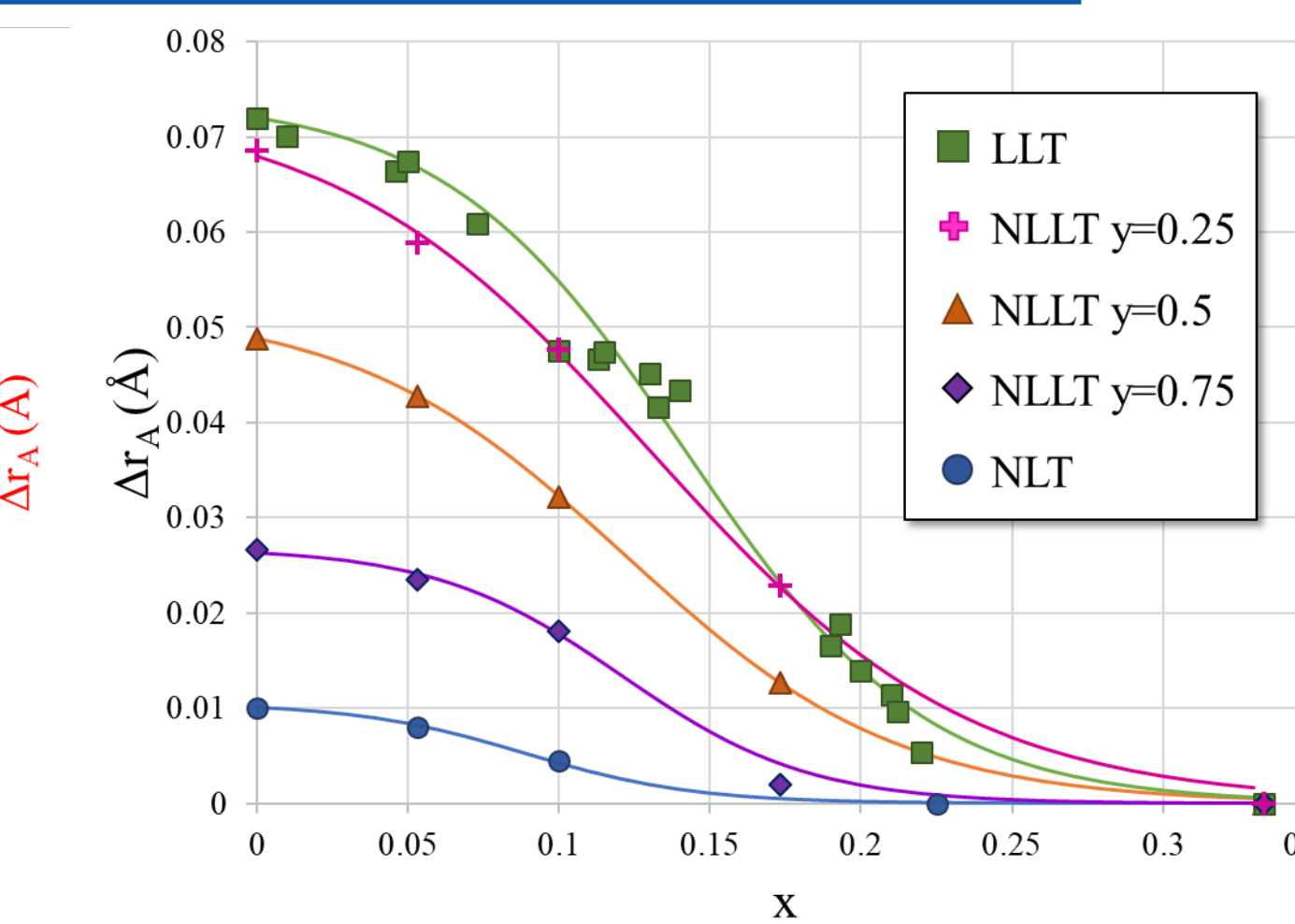


Figure 11:  $\text{Na}_{(1-3x)/4}\text{La}_{(1+x)/2}\text{TiO}_3$  (blue),  $(\text{Na}_y\text{Li}_{1-y})_{(1-3x)/4}\text{La}_{(1+x)/2}\text{TiO}_3$  ( $y=0.75$ , purple), ( $y=0.50$ , orange), ( $y=0.25$ , pink), and  $\text{Li}_{(1-3x)/4}\text{La}_{(1+x)/2}\text{TiO}_3$  (green)<sup>[2]</sup> A-site size adjustment factors as functions of vacancy concentration from experimentally collected data.

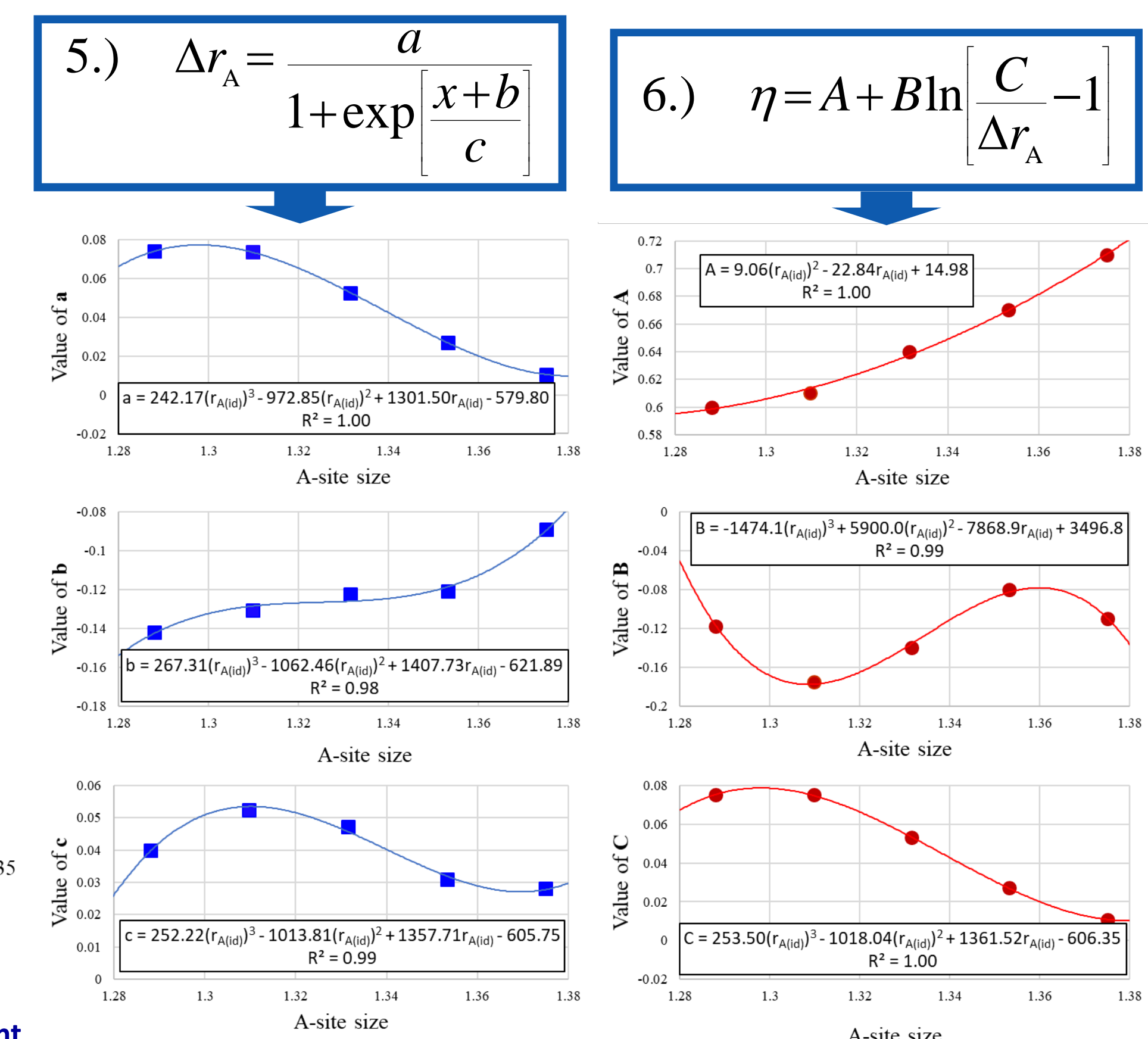


Figure 12: Coefficients of equation (5) (blue squares) as functions of A-site size and coefficients of equation (6) (red circles) as functions of A-site size.

## Conclusion

$(\text{Na}_y\text{Li}_{1-y})_{(1-3x)/4}\text{La}_{(1+x)/2}\text{TiO}_3$  and  $\text{Ba}(\text{Mg}_{1/3}\text{Ta}_{2/3})\text{O}_3$  were synthesized using traditional ceramic techniques. Empirical models which allow for the prediction of A-site and B-site order parameters using easily obtainable experimental data were made for layered type ordering on the A site and rocksalt type ordering on the B site. The models also allow for the prediction of the A-site and B-site correction parameters ( $\Delta r_A$  and  $\Delta r_B$ ) using vacancy concentration and sintering time, respectively. These models could potentially be extended in order to enable the prediction of ordering parameters in other complex perovskite systems from ionic radii data and experimentally-derived pseudocubic lattice constants alone.

[3] E. Smith, K. Tolman, R. Ubic, An empirical model for B-site cation ordering in  $\text{Ba}(\text{Mg}_{1/3}\text{Ta}_{2/3})\text{O}_3$ , J. Alloys Compd. 735 (2018) 2356-2362.

## Acknowledgements

The authors are grateful to Dr. Karthik Chinnathambi of the BSCMC for help with analyzing XRD patterns, TEM specimen preparation, and analyzing electron diffraction patterns.